Available online at www.sciencedirect.com
SCIENCE DIRECT®
Journal of Molecular Structure 700 (2004) 3–12
Journal of MOLECULAR STRUCTURE
www.elsevier.com/locate/molstruc

Low-temperature NMR spectra of fluoride–acetic acid hydrogen-bonded complexes in aprotic polar environment

Nikolai S. Golubev[a], Peter M. Tolstoy[a,b], Sergei N. Smirnov[a], Gleb S. Denisov[a], Hans-Heinrich Limbach[b,*]

[a]*V.A. Fock Institute of Physics, St Petersburg University, Ulyanovskaja 1, Peterhof, Russian Federation*
[b]*Institut fuer Chemie der Freien Universitaet Berlin, Takustrasse 3, D14195 Berlin, Germany*

Received 20 January 2004; revised 20 January 2004; accepted 21 January 2004

Abstract

Using low-temperature NMR (^{1}H, ^{19}F) technique in the slow exchange regime, the solutions containing tetrabutylammonium (TBA) acetate and HF have been studied in an aprotic freon mixture, CDF_3/CDF_2Cl, exhibiting a dielectric permittivity, which increases strongly by lowering the temperature. Two different hydrogen bonded anionic clusters, a 1:1 cluster of the type $AcO^{\delta-}\cdots H\cdots F^{-1+\delta+}$ ($[AcOHF]^-$) and a 2:1 cluster of the type $AcOH\cdots F^-\cdots HOAc$ ($[(AcOH)_2F]^-$) have been detected in equilibrium with each other, both forming ion pairs with the TBA countercation. $[AcOHF]^-$ exhibits an extremely strong hydrogen bond, with a proton shared between partially negatively charged oxygen and fluorine atoms. The NMR chemical shifts and scalar spin–spin coupling constants, $^1J(FH)$, have been measured in the temperature range between 110 and 160 K, where separate NMR signals are observed for both species. In addition, H/D isotope effects on the ^{19}F NMR chemical shielding have been measured for both clusters.

In contrast to the related complexes $[(FH)_nF]^-$ ($n = 1-4$) studied previously, the NMR parameters of $[AcOHF]^-$ and of $[(AcOH)_2F]^-$ depend strongly on temperature. This effect is associated with the increasing polarity of the solvent with decreasing temperatures, established earlier, which displaces the proton from fluorine to oxygen. As a motive power of this conversion, preferential solvation of the compact fluoride ion as compared to acetate is proposed.

Keywords: Low-temperature NMR; Hydrogen bond; Isotope effect; Acetic acid; Fluoride anion

1. Introduction

Strong and short ('low-barrier') hydrogen bonds in charged (anionic or cationic) complexes (clusters) have attracted recently the attention of many biochemists due to presumed role of these bonds in enzymic catalysis [1–11]. One of the main questions when invoking the concept of low-barrier hydrogen bonding to biochemical reactions is how these bonds are affected by the surrounding water molecules or other polar groups. In fact, the problem of how solvent polarity influences the length, strength and symmetry of a short hydrogen bond in charged complex has discussed in the literature for a long time. Some experimental and theoretical results are in favour of solvent assisted hydrogen bond weakening, lengthening and asymmetrization, which makes the participation of such bonds in enzymic processes doubtful [12]. On the other hand, in some recent studies [13–15] it was shown that hydrogen bonds in homoconjugated anions are strengthened and contracted by embedding into a polar medium. This finding is in agreement, in particular, with the increase of the scalar $^{2h}J(FHF)$ spin coupling constant between fluorine nuclei across the hydrogen bonds with increasing polarity of the solvent for the dihydrogen trifluoride ion, which exhibits two coupled short hydrogen bonds of the type $[F-H\cdots F\cdots H-F]^-$ [16,17]. A simple explanation of this effect was proposed, i.e. that the electrostatic repulsion between negatively charged fluorine atoms is reduced by a medium of high dielectric constant ε [15].

Taking in mind, that a solvent may act on H-bonds of different type in different ways, in this communication we

* Corresponding author. Tel.: +49-30-8385-5375; fax: +49-30-8385-5310.
E-mail addresses: limbach@chemie.fu-berlin.de (H.-H. Limbach), nick.golubev@pobox.spbu.ru (N.S. Golubev), tolstoy@chemie.fu-berlin.de (P.M. Tolstoy).

0022-2860/$ - see front matter © 2004 Elsevier B.V. All rights reserved.
doi:10.1016/j.molstruc.2004.01.024

describe the influence of the solvent polarity on the NMR parameters of ionic clusters with strongly asymmetric hydrogen bonds, formed by hydrogen fluoride with the acetate-anion, in ion pairs with the 'inert' tetrabutylammonium (TBA) counter cation. As described in our previous papers [18–20], we took advantage of a very strong dependence of ε of the low-freezing solvent CDF_3/CDF_2Cl on temperature. According to Ref. [18], ε of this mixture rises rapidly from about 25 to 45 when temperature is decreased from 170 to 100 K. This makes it possible to study the dependence of the NMR parameters as a function of ε without changing the solvent. At temperatures as low as 100–170 K, the slow hydrogen bond exchange regime is usually reached where NMR signals of different acid–base complexes being in equilibrium with each other are well resolved, a circumstance which increases considerably the informative power of liquid state NMR. As a result of this work, we succeeded in finding and assigning NMR features of several hydrogen-bonded species being present in the solutions in chemical equilibrium, in the slow hydrogen bond exchange regime. In this communication, the spectra of two of them, namely, $AcO^{\delta-}\cdots H\cdots F^{-1+\delta+}$ ($[AcOHF]^-$) and $AcOH\cdots F^-\cdots HOAc$ $[(AcOH)_2F]^-$ are described and characterized.

2. Experimental

2.1. Materials

A measured amount of 40% hydrofluoric acid was added to a solution of TBA acetate (Aldrich) in dichloromethane (Aldrich). Then water was removed by repeated azeotropic distillation with dry dichloromethane. The H/D replacement of the mobile (OH, FH) proton was performed by dissolving a salt in methanol–OD: proton/deuterium exchange between acetic acid–fluoride anion and excess of methanol leads to the partial substitution of H for D in the salt. Methanol was then removed under reduced pressure, leaving in the deuterated salt in the flask. The oily product was placed into a hermetic thick-walled NMR sample tube equipped with PTFE (polytetrafluoroethylene) valves (Wilmad, Bueno), connected to a high vacuum line and filled with the solvent via vacuum transfer. The solvent, CDF_3/CDF_2Cl, with freezing point below 100 K was added to the samples by vacuum transfer. The approximate overall concentration of the samples, estimated by weighing chemicals and measuring the volume of the solution at low temperatures (around 120 K), was about 0.02 M.

2.2. NMR spectra

The Bruker AMX-500 NMR spectrometer used was equipped with a low-temperature probe-head which allowed us to perform experiments down to 100 K. ^1H and ^{19}F NMR chemical shifts were measured using fluoroform, CHF_3 (CDF_3), as internal standard, and were converted to the conventional TMS (tetramethylsilane) scale. The total deuterium fraction was determined by comparison of the integrated signal intensity of the residual mobile proton site with those of the immobile CH-protons. It should be noted that, as a rule, the resolution in our low-temperature spectra is much worse than in usual (ambient temperature) liquid state spectra. It is explained by a considerable viscosity of freon mixtures, and is markedly revealed in spectra of nuclei with high magnetic shielding anisotropy, like ^{19}F.

3. Hydrogen bond correlations

In order to link the NMR parameters of the hydrogen bonded FHO and OHFHO systems studied to hydrogen bond geometries we will make use of several hydrogen bond correlations, which have been established previously by various authors.

To a given hydrogen bond of the type A–H···B one can normally associate two distances, r_1 for the diatomic unit AH and r_2 for the diatomic unit H···B. According to Pauling [21], these distances correspond to the valence bond orders

$$p_1 = \exp\{-(r_1 - r_1^0)/b_1\},$$
$$p_2 = \exp\{-(r_2 - r_2^0)/b_2\}, \text{ with } p_1 + p_2 = 1. \quad (1)$$

For H, the total valence has to be unity. The correlation of r_1 with r_2 also implies a correlation between the hydrogen bond coordinates $q_1 = 1/2(r_1 - r_2)$ and $q_2 = r_1 + r_2$. For a linear hydrogen bond, q_1 represents the distance of H from the hydrogen bond center and q_2 the distance between atoms A and B. When H is transferred from one heavy atom to the other, q_1 increases from negative values to positive values. q_2 goes through a minimum which is located at $q_1 = 0$ for AHA and near 0 for AHB systems. The parameters in Eq. (1) have been derived empirically from various experiments such as neutron diffraction or solid state NMR and the results of quantum-mechanical calculations. For the FH and OH bonds, the following parameters have been proposed [17,19], i.e.

$$r_1^0 = 0.897 \text{ Å and } b_1 = 0.360 \text{ Å for HF and}$$
$$r_2^0 = 0.942 \text{ Å}, \; b_2 = 0.371 \text{ Å for OH.} \quad (2)$$

r_1^0 and r_2^0 refer to the values of the hypothetical diatomic molecules. b_1 and b_2 describe the decrease of the bond orders with increasing distances.

For the correlation of HF coupling constants in FHB systems, some of us have proposed the relation [20]

$$^1J(FH\text{B}) = {}^1J(FH)^0 p_{\text{FH}} - 8\Delta J(FH\text{B}) p_{\text{FH}} p_{\text{HB}}^2,$$
$$^1J(FH)^0 = 600 \text{ Hz}, \quad (3)$$

with $\Delta J(FH\mathrm{B}) = 162.5$ Hz for B = F and $\Delta J(FH\mathrm{B}) = 190$ Hz for B = N. We will assume later that the average value is valid for B = O, $\Delta J(FHO) = 176$ Hz.

For the analysis of the ^{1}H chemical shifts we use the relation

$$\delta(\mathrm{F}H) = \delta(\mathrm{F}H)^0 p_{\mathrm{FH}} + \delta(H\mathrm{B})^0 p_{\mathrm{HB}} + 4\Delta\delta(\mathrm{F}H\mathrm{B}) p_{\mathrm{FH}} p_{\mathrm{HB}} \quad (4)$$

with $\Delta\delta(\mathrm{F}H\mathrm{B}) = 15.2$ ppm. For B = F, we assume a value of $\delta(\mathrm{F}H)^0 = \delta(H\mathrm{F})^0 = 0$ ppm, and for B = O that $\delta(H\mathrm{O})^0 = 6$ ppm, referring to free HF and acetic acid molecules.

For the fluorine chemical shifts we assume that

$$\delta F = \delta(F\mathrm{H})^0 p_{\mathrm{FH}} + \delta F^{\infty} p_{\mathrm{HB}} + 8\Delta\delta(F\mathrm{HB}) p_{\mathrm{FH}} p_{\mathrm{HB}}^2 \quad (5)$$

Here, we set for B = O $\Delta\delta(F\mathrm{HO}) = 100$ ppm, $\delta(F)^{\infty} = -100$ ppm and $\delta(F\mathrm{H})^0 = -210$ ppm.

We note that these parameters are not 'hard' parameters but may change, when further experimental and theoretical results will be available. Therefore, one has to keep in mind that geometries derived using these equations from NMR parameters might be subject to systematic errors. However, they are sufficient for qualitative comparison of different H-bonded systems.

Finally, we assume the following relations between the valence bond orders of the deuterated and the protonated hydrogen bonds

$$\begin{aligned} \Delta p =& p_{\mathrm{FH}} - p_{\mathrm{FD}} - (p_{\mathrm{OH}} - p_{\mathrm{OD}}) = \\ & A(p_{\mathrm{FH}} p_{\mathrm{OH}})^B (p_{\mathrm{FH}} - p_{\mathrm{OH}}), \\ & p_{\mathrm{FH}} + p_{\mathrm{OH}} = p_{\mathrm{FD}} + p_{\mathrm{OD}} = 1. \end{aligned} \quad (6)$$

The parameters A and B are empirical and will depend on the type of the hydrogen bond studied. We will use here the values $A = 220$ and $B = 5$ for the FHF and the FHO hydrogen bonded systems considered in this work. For a given set of values p_{FH} and p_{OH} one can calculate using Eq. (6) the corresponding values of p_{FD} and p_{OD} and hence the fluorine chemical shifts of the deuterated systems. For this purpose, an appropriate simple computer program was written.

4. Results

4.1. NMR spectra at 120 K

In Fig. 1 are depicted the low-field ^{1}H NMR signals of solutions TBA^+ acetate (AcO^-) with hydrogen fluoride, with acetate/HF ratios of 3:1 (top) and 3:2 (bottom) and the deuterium fractions $x_D = 0$ (top) and $x_D = 0.7$ (bottom) in the hydrogen bonded sites.

The upper spectrum exhibits two intense singlets at 19.3 and 16.5 ppm, which are typical for the acetic acid–acetate homoconjugated anions labeled here as $[OHO]^-$ and $[OHOCOHO]^-$. These anions have been characterized recently; they are subject to a fast acetate–acetic acid interconversion as revealed by ^{13}C NMR [19]. In addition, we find two doublets, exhibiting chemical shifts of 18.33 and 15.58 ppm and spin–spin coupling constants $^1J(FH)$ near 60 Hz at 120 K. These signals were assigned to the anions $[\mathrm{AcOHF}]^- \equiv [\mathrm{FHO}]^-$ and $[(\mathrm{AcOH})_2\mathrm{F}]^- \equiv [\mathrm{OHFHO}]^-$ as indicated in Fig. 1. As shown in the lower spectrum, two new signals appear at

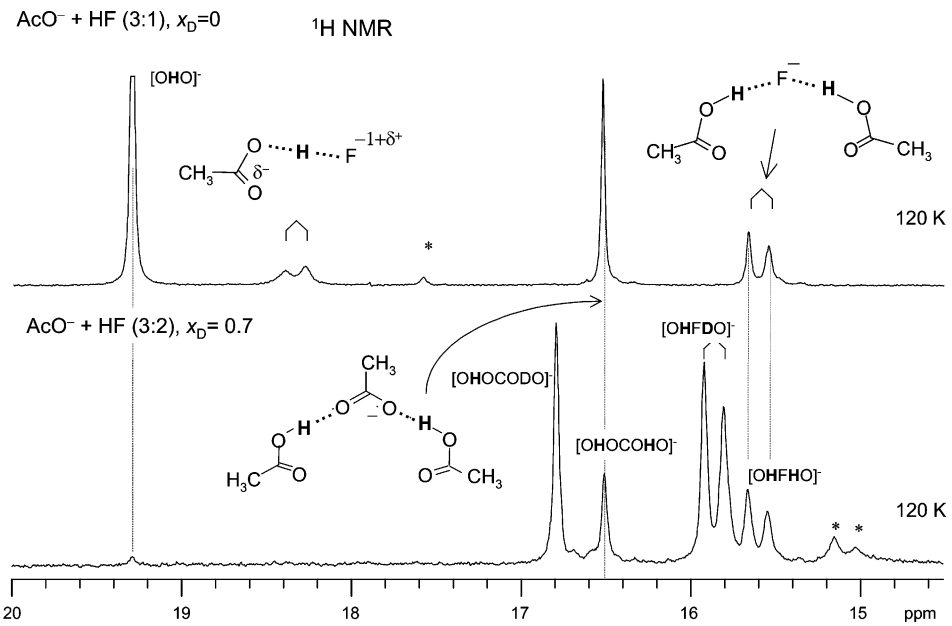

Fig. 1. Low-field part of ^{1}H NMR spectra of solutions of tetrabutylammonium acetate and hydrogen fluoride in CDF_3/CDF_2Cl at 120 K. Top: molar ratio 3:1, deuterium fraction in the hydrogen bond sites $x_D = 0$. Bottom: molar ratio 3:2, $x_D = 0.7$.

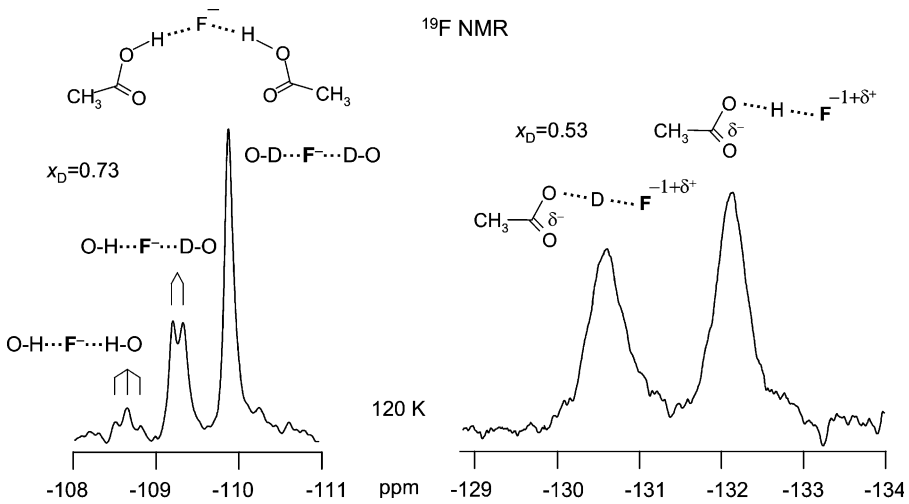

Fig. 2. ^{19}F NMR signals of solutions of tetrabutylammonium acetate and hydrogen fluoride (molar ratio 3:2) in CDF_3/CDF_2Cl at 120 K. Left: signals of $[OHFHO]^-$, L = H, D at $x_D = 0.73$. Right: signals of $[FHO]^-$ at $x_D = 0.53$.

16.8 and 15.84 ppm after partial deuteration, assigned to the complexes $[OHOCODO]^-$ and $[OHFDO]^-$.

The assignment of $[OHO]^-$ and $[OHOCOHO]^-$ was based on the following observations: (i) a decrease of the acetate/HF ratio reduces the intensity of the low-field signal, and that of the high-field one is increased; (ii) partial H/D replacement does not alter the type of the low-field signal, but produces a new peak for $[OHOCODO]^-$ as mentioned above. This isotope shift has been labeled as a geometric 'vicinal' isotope effect [19].

The assignment of the fluorine containing species was done in a similar way. When the acetate/HF ratio is decreased, the intensity of the low-field signal decreases, thus this signal has to be assigned to $[FHO]^-$ and the high field signal to $[OHFHO]^-$. Again, partial H/D substitution reduces the intensity of the $[FHO]^-$ signal, and introduces a new ^{1}H signal for $[OHFDO]^-$. The situation is analogous to the corresponding homoconjugate acetate–acetic acid anions.

Some typical ^{19}F signals of samples partially deuterated in the hydrogen bond sites are depicted in Fig. 2. Signals of 1:1 complexes $[FHO]^-$ and $[FDO]^-$ are assigned by varying the deuterium fraction. The signals are broad and a scalar coupling with H is not resolved in the case of $[FHO]^-$. The origin of this effect will be discussed later.

The ^{19}F signals of $[OHFHO]^-$, $[OHFDO]^-$ and $[ODFDO]^-$ are sharper, and appear at lower field as indicated in Fig. 2. Only $[OHFHO]^-$ and $[OHFDO]^-$ exhibit a triplet and a doublet splitting with $^1J(FH)$ coupling constants of about 60 Hz as expected from the ^{1}H spectra. Deuteration leads to a successive high-field shift. Scalar couplings to D which should be of the order of 9 Hz are not resolved.

All NMR parameters are collected in Table 1.

4.2. Variable temperature NMR spectra

In order to elucidate the effect of temperature on the NMR parameters of the $[FHO]^-$ and $[OHFHO]^-$ clusters we have performed variable temperature measurements on samples of TBA acetate and HF mixture in CDF_3/CDF_2Cl which are depicted in Figs. 3 and 4. The ^{1}H doublet of $[FHO]^-$ shifts downfield and the one of $[OHFHO]^-$ upfield as temperature is decreased; at the same time the $^1J(FH)$ splitting decreases. Both signals exhibit differential line widths of the doublet signal components, which are more pronounced at low temperatures. Generally, asymmetric doublets are caused by an interference between dipolar and chemical shift anisotropy relaxation mechanisms and an increase of the rotational correlation times τ. For HF doublets, the low-field component is broader than the high-field component if the coupling constant $^1J(FH)$ is positive and the high-field component is broader than the low-field

Table 1
Experimental NMR parameters of the 1:1 and 2:1 complexes of acetic acid with fluoride in CDF_3/CDF_2Cl at 120 K

NMR parameter	$[OHF]^-$	$[OHFHO]^-$
δ(F*H*O) ± 0.005 (ppm)	18.327	
^1J(*FH*O) ± 0.5 (Hz)	61.0	
δ(*F*HO) ± 0.01 (ppm)	−132.21	
δ(*F*DO) ± 0.01 (ppm)	−130.73	
δ(O*H*FHO) ± 0.01 (ppm)		15.58
δ(O*H*FDO) ± 0.01 (ppm)		15.84
^1J(O*HF*HO) ± 0.5 (Hz)		−60.5
^1J(O*HF*DO) ± 0.5 (Hz)		−60.5
δ(OH*F*HO) ± 0.01 (ppm)		−108.64
δ(OH*F*DO) ± 0.01 (ppm)		−109.26
δ(OD*F*DO) ± 0.01 (ppm)		−109.90

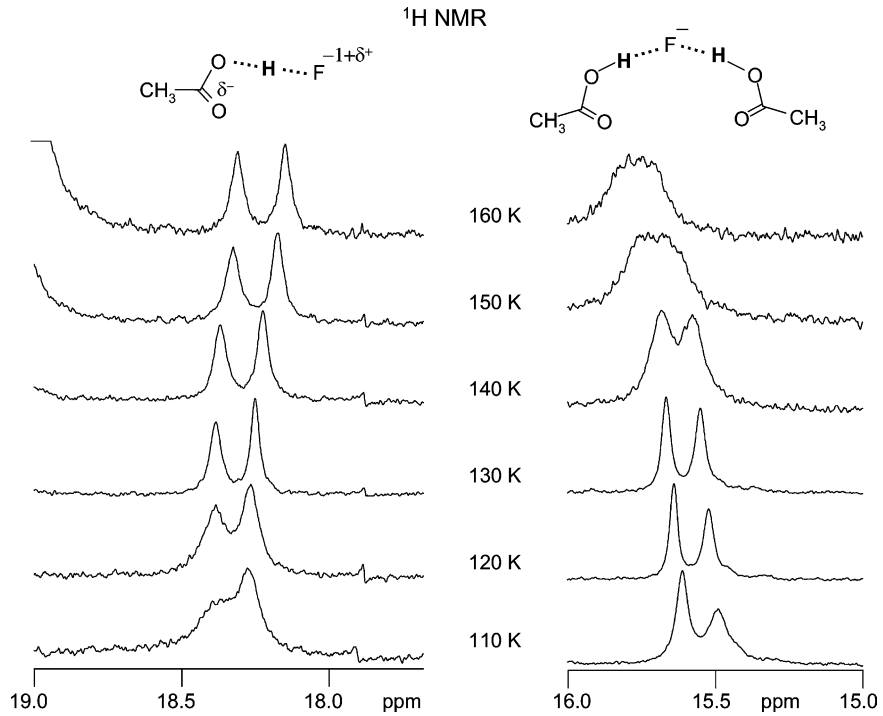

Fig. 3. Variable temperature ^{1}H NMR signals of $[FHO]^-$ (left) and $[OHFHO]^-$ (right) dissolved in CDF_3/CDF_2Cl. For further explanation see text.

component if $^1J(FH)$ is negative, as discussed previously [16,20]. Thus, we conclude that $^1J(FHO) > 0$ and $^1J(OHF\ HO) < 0$. At high temperatures, the line widths of the $[OHFHO]^-$ species are larger than those of $[FHO]^-$, a phenomenon which has to be assigned to the onset of hydrogen bond and proton exchange. At lower temperatures, the situation is inversed. Thus, $[FHO]^-$ seems to be involved in a so far unresolved dynamic process.

This process is better resolved in the ^{19}F signals of this species, depicted in Fig. 4. The hydrogen bond exchange between the $[FHO]^-$ and for $[FDO]^-$ species is slow in the NMR time scale at the highest and lowest temperature accessible, and sharp lines are observed in both limits. At 170 K, doublet $[FHO]^-$ is observed arising from scalar $^1J(FH)$ coupling. The splitting decreases with decreasing temperatures. Around 150 K, the lines are broadened and are shifted to low-field. A maximum broadening is observed around 130 K, and then again a sharpening of the lines below this temperature.

It is unlikely that these spectral features arise from transverse relaxation phenomena, for example from an increase of the fluorine magnetic shielding anisotropy, effective especially at 130 K. By contrast, these spectral features are typical for the presence of an equilibrium between two species **A** and **B**, where **A** dominates at high and **B** at low temperatures, where the equilibrium constant is given by $K = x_B/x_A = k_{AB}/k_{BA}$. x_A and x_B are the mole fractions of both species and k_{AB} and k_{BA} are the first-order or pseudo-first-order rate constants of the interconversion. At 130 K, both

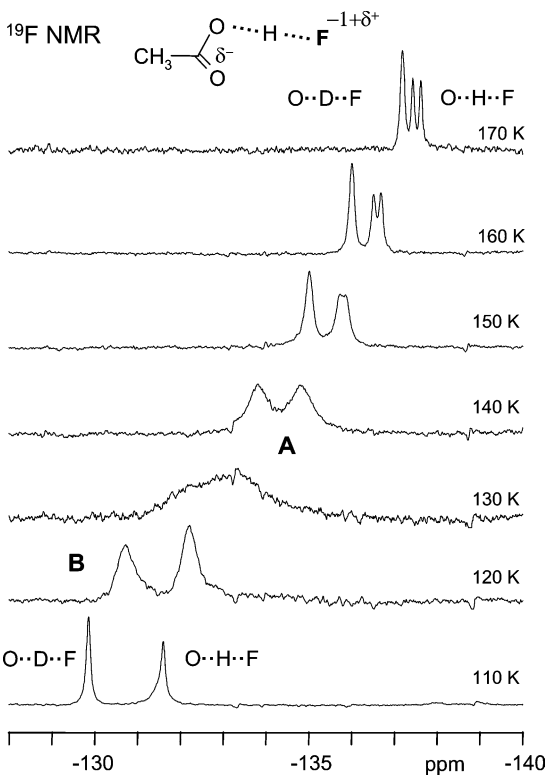

Fig. 4. Variable temperature ^{19}F NMR signals of a mixture of $[OHF]^-$ and $[ODF]^-$ in CDF_3/CDF_2Cl. For further explanation see text.

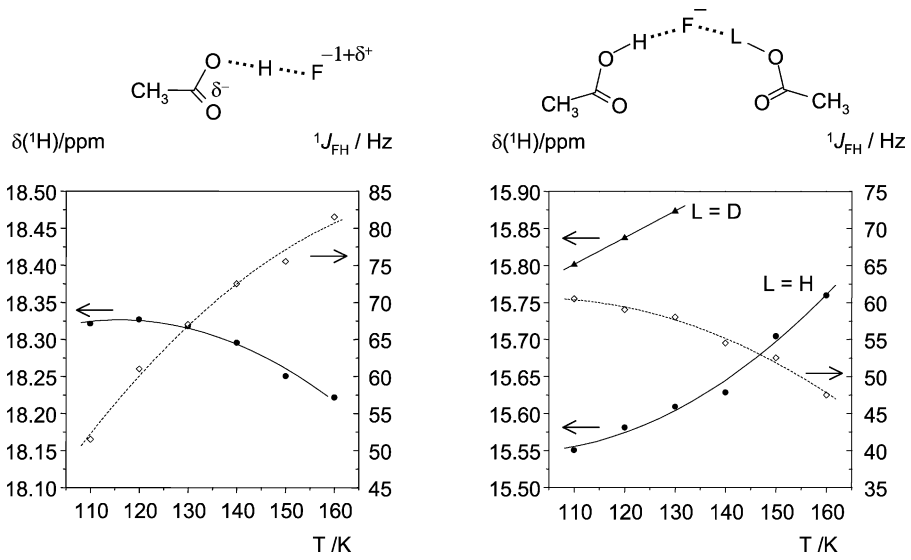

Fig. 5. Dependencies of the measured NMR parameters (chemical shifts and scalar spin–spin coupling constants) for two clusters, $[FHO]^-$ (left) and $[OHFHO]^-$ (right), on temperature in the region, 110–160 K.

species exhibit similar mole fractions, and in addition, the exchange rate constants $k_{AB} \approx k_{BA}$ are by chance of the order of the chemical shift difference in Hz of the exchanging species, $\pi(\nu_A - \nu_B)$. As the values of ν_i are temperature dependent, we did not try to perform a quantitative line shape analysis. However, for 130 K we can estimate $k_{AB} \approx k_{BA} \approx \pi(\nu_A - \nu_B)$ roughly to be about 300 s^{-1}. We note that this interconversion does neither lead to a collapse of spin–spin splitting nor of the isotope splitting. This means, that the process does not involve proton nor hydrogen bond exchange. On the other hand, we note that the equilibrium constant K has to change strongly with temperature in order to produce a complete transformation of form **B** to form **A** within 20 K. This indicates a very large negative entropy and a very large negative enthalpy of the transition **A** → **B**.

Finally, in Fig. 5 we have plotted the ^1H chemical shifts and $^1J_{HF}$ coupling constants of $[FHO]^-$, $[OHFHO]^-$ and $[OHFDO]^-$ as a function of temperature.

Data points for all variable temperature experiments are collected in Tables 2 and 3.

5. Discussion

The above results show that acetic acid and fluoride anion can form 1:1 and 2:1 clusters in polar solvent such as CDF_3/CDF_2Cl. In this section, we will first link the NMR parameters of these clusters with the corresponding hydrogen bond geometries. We will then discuss the effects of H/D substitution as well as temperature dependent solvation on these geometries, in comparison with the clusters of HF with fluoride, which have been studied previously [16,17]. Finally, the nature of the dynamic process in which the 1:1 complex is involved is discussed.

Table 2
^1H NMR parameters of the 1:1 and 2:1 complexes of acetic acid with fluoride, $[FHO]^-$, $[OHFHO]^-$ and $[OHFDO]^-$, in CDF_3/CDF_2Cl as a function of temperature

T (K)	$[FHO]^-$				$[OHFHO]^-$				$[OHFDO]^-$			
	δ(F*H*O) (ppm)	$^1J(FHO)$ (Hz)	W_1 (Hz)	W_2 (Hz)	δ(F*H*O) (ppm)	$^1J(FHO)$ (Hz)	W_1 (Hz)	W_2 (Hz)	δ(F*H*O) (ppm)	$^1J(FHO)$ (Hz)	W_1 (Hz)	W_2 (Hz)
110	18.322	51.5	80	38	15.55	−60.5	24	40	15.80	61.0	25	50
120	18.327	61.0	43	35	15.58	−59.0	16	21	15.84	59.0	16	26
130	18.318	67.0	23	18	15.61	−58.0	18	21	15.87	57.0	27	31
140	18.296	72.5	27	23	15.63	−54.5	42	46				
150	18.251	75.5	28	24	15.71	−52.5	70	70				
160	18.222	81.5	25	23	15.76	−47.5	70	70				

δ(F*H*O), chemical shift of the H-bond proton; W_1, signal line width in Hz of the low-field; W_2, of the high-field component.

Table 3
^{19}F NMR parameters of the 1:1 acetate–HF complex $[FHO]^-$ in CDF_3/CDF_2Cl as a function of temperature

T (K)	H form		D form		$\delta(FDO) - \delta(FHO)$ (ppm)
	$\delta(FHO)$ (ppm)	W (Hz)	$\delta(FDO)$ (ppm)	W (Hz)	
110	−131.60	78	−129.86	54	1.74
120	−132.21	199	−130.73	196	1.49
130	−133.47	428	−132.21	566	1.26
140	−134.82	344	−133.81	213	1.01
150	−135.80	145	−135.02	93	0.78
160	−136.60	50	−136.01	64	0.59
170	−137.53	35	−137.19	46	0.34

W, signal line width.

5.1. Hydrogen bond geometries of $[FHO]^-$ and $[OHFHO]^-$ and their deuterated isotopologs

In Fig. 6 we have depicted various geometric and NMR hydrogen bond correlations of the $[FHO]^-$ and $[OHFHO]^-$ clusters studied here. For comparison, we have included those published previously for various hydrogen fluoride–fluoride anions, $[(FH)_nF]^-$, where $n = 1–4$.

In Fig. 6a and f are depicted the correlations of the hydrogen bond coordinate, $q_1 = 1/2(r_1 - r_2)$ with $q_2 = r_1 + r_2$. As has been shown previously [16,17], the values obtained by ab initio calculations for $[(FH)_nF]^-$ are well located on the correlation curve, represented by the solid line in Fig. 6a. The geometric data in Fig. 6f were obtained empirically as described below.

In Fig. 6b and g are depicted the values of the coupling constants $^1J(FHB)$, B = F, O as a function of q_1. As described previously both for FHF and FHN systems, a change of the sign of $^1J(FHB)$ is observed when H moved away from F just after crossing the H-bond center. After reaching a minimum, the coupling constants go to 0, because the FH distance becomes larger (obviously, the coupling constant is 0 at infinite distance). In the case of the FHN systems we observed recently that the minimum was deeper as compared to FHF [20]. The same is true in the case of $[FHO]^-$ and $[OHFHO]^-$, we observe a similar sign change: the values of $^1J(FHO)$ are positive for $[FHO]^-$ and negative for $[OHFHO]^-$. The minimum value is again larger than the one for FHF. Assuming the validity of

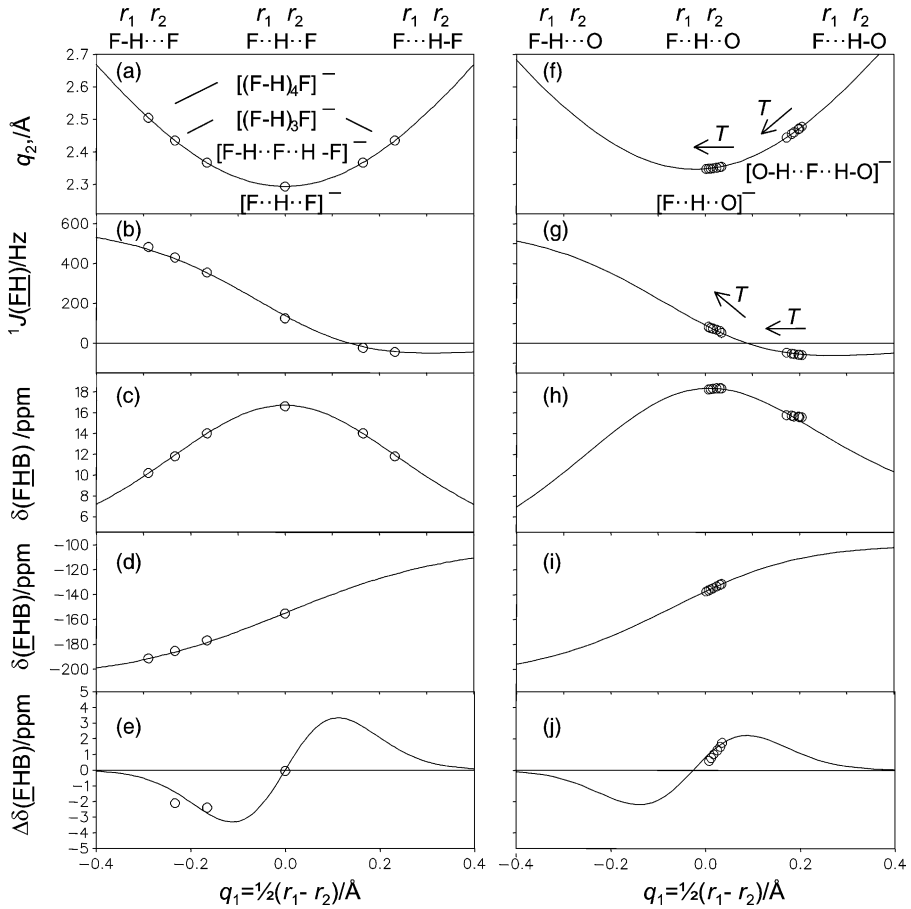

Fig. 6. Hydrogen bond correlations of clusters of $[(FH)_nF]^-$ (left), adapted from Ref. [17] and of $[FHO]^-$ and $[OHFHO]^-$ (right). The solid lines correspond to the equations listed in the hydrogen bond correlations section. For further explanation see text.

Eq. (3), we obtain the solid line of Fig. 6g. Now, we could adjust the values of q_1 in such a way that the experimental values of $^1J(FHO)$ are located on the correlation curve. Fixing the values of q_1 determined also those of q_2 in Fig. 6f.

In Fig. 6c and h are depicted the ^{1}H chemical shifts of both types of systems, and the agreement with Eq. (4) is satisfactory. In Fig. 6d and i we have included the corresponding fluorine chemical shifts. As these shifts are much more sensitive to the hydrogen bond geometries, they were used to fine tune the q_1 values. The H/D isotope effects on the fluorine chemical shifts, $\Delta\delta(F\text{HB}) = \delta(F\text{DB}) - \delta(F\text{HB})$ are included in Fig. 6e and j. They are well reproduced by the solid lines calculated using Eq. (6). Again, the data for the FHF system were taken from Ref. [17].

We note that the $\Delta\delta(F\text{HF})$ values are negative for H close to F, and even for $[FHF]^-$ a negative value of -0.32 ppm was found. In our case, the values for $[FHO]^-$ are positive, a result which can be taken as indication that H is a little bit closer to O than to F, although Fig. 6 indicates that $[FHO]^-$ is very similar to the symmetric $[FHF]^-$. By increasing temperature, the hydron in $[FHO]^-$ is shifted towards F, and at 160–170 K, a symmetric proton shared geometry is reached. Note, that there are no unusual spectral changes in this temperature region, which is not surprizing while for the asymmetric hydrogen bonds $q_1 = 0$ does not correspond to any special physical situation. By contrast, the hydrons in $[OHFHO]^-$ are closer to O than to the central fluoride, in a similar way as in the corresponding cluster $[FHFHF]^-$. Again, increasing temperature shifts both H towards F, but the centered H-bond is not reached at 160 K. As a motive power of this displacement, preferential solvation of compact fluoride anion as compared to the acetate is proposed. All hydrogen bond distances estimated from the analysis of Fig. 6 are included in Table 4. These distances are affected by systematic errors, in view of many assumptions both concerning the forms of Eqs. (1)–(6) as well as the parameters used. However, we think that relative changes are well reproduced, in particular the observed sign change of the coupling constants.

The reasons for the temperature shifts have been discussed in previous papers [18–20]. As temperature is lowered, the local polarity increases because of solvent ordering around the solutes, and structures with larger dipole or quadrupole moments are favoured. In non-charged 'neutral' hydrogen bonds, the zwitterionic structures are reached by shifting the proton towards or across the hydrogen bond center. In the case of ions, a non-symmetrical charge distribution will lead to similar effects. The geometric changes of $[FHO]^-$ with temperature as expressed in Fig. 6 and Table 4 are then the consequence of this phenomenon.

Finally, we come to the discussion of the vicinal isotope effects [19,20] found previously for $[FHFHF]^-$ and the $[OHOCOHO]^-$ systems, and here for $[OHFHO]^-$. This phenomenon implies that the chemical shift difference $\delta(\text{A}H\text{XDB}) - \delta(\text{A}H\text{XHB})$ of a coupled hydrogen bonded system AHXHB is non-zero. This means that the chemical shift of H in AHX depends on whether the neighbouring bond XHB is protonated or deuterated. For $[OHOCOHO]^-$ a value of $+0.29$ ppm was found (see Fig. 1 and Ref. [19]), a value which is very close to the one of 0.26 observed for $[OHFHO]^-$ (Fig. 1 and Table 1). For comparison, the value of $[FHFHF]^-$ is 0.155 ppm. These values indicate a mutual influence of the two coupled hydrogen bonds in all the three systems which exhibit an anti-cooperativity. Thus, deuteration of XHB leads to an increase of the X···B distance, but a decrease of the A···X distance. In the case of anions, this feature is understandable and in terms of a higher charge on X as compared to A and B. When the donor HB moves away from X^-, the latter becomes more 'basic' and attracts the proton from AH, leading then to a distance increase of AH and a shortening of the A···X distance. Thus, from vicinal isotope effects qualitative conclusions about the hydrogen bond structure can be obtained.

Table 4
Hydrogen bond distances of $[FHO]^-$ and $[OHFHO]^-$ obtained by NMR

Species	T (K)	r_{FH} (Å)	q_2 (Å)	q_1 (Å)	r_{OH} (Å)
$[OHF]^-$	110	1.212	2.234	0.035	1.142
$[OHF]^-$	120	1.208	2.353	0.031	1.145
$[OHF]^-$	130	1.200	2.351	0.024	1.151
$[OHF]^-$	140	1.192	2.350	0.017	1.158
$[OHF]^-$	150	1.186	2.349	0.012	1.162
$[OHF]^-$	160	1.181	2.348	0.007	1.167
$[OHF]^-$	170	1.176	2.347	0.002	1.171
$[ODF]^-$	110	1.206	2.353	0.030	1.147
$[ODF]^-$	120	1.201	2.351	0.025	1.151
$[ODF]^-$	130	1.191	2.349	0.016	1.158
$[ODF]^-$	140	1.181	2.348	0.007	1.167
$[ODF]^-$	150	1.174	2.347	0.001	1.173
$[ODF]^-$	160	1.169	2.346	−0.004	1.178
$[OHFHO]^-$	110	1.444	2.477	0.205	1.034
$[OHFHO]^-$	120	1.436	2.472	0.200	1.036
$[OHFHO]^-$	130	1.432	2.469	0.198	1.037
$[OHFHO]^-$	140	1.418	2.460	0.188	1.041
$[OHFHO]^-$	150	1.410	2.455	0.183	1.044
$[OHFHO]^-$	160	1.395	2.444	0.173	1.049

5.2. Structure and dynamics of $[FHO]^-$ at low-temperature

So far, we have only considered the geometry of the hydrogen bond in $[FHO]^-$ but did not yet discuss the whole structure of this complex, which is characterized also by an orientational degree of freedom of the acetate moiety with respect to the HF moiety. In fact, using different techniques, rotational isomers have been detected previously for formic acid monomer in gas phase and for the complex of formic acid with hexamethylphosphorotriamide in polar solvents [22,23].

The rotational isomerism may be characterized by different COF angles β as depicted in Scheme 1 for two

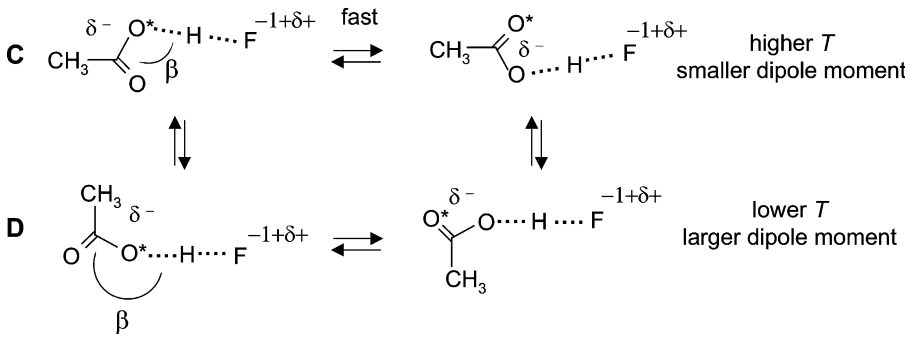

Scheme 1.

arbitrary values of β leading to two isomers **C** and **D**. Naturally, one could equally well conceive a broad distribution of angles β. The different configurations will exhibit different electrical properties, and therefore, by the interaction with the surrounding solvent molecules and the countercation isomers with larger dipole moments will be favoured at lower temperatures.

Another degree of freedom arises from the possibility of a hydrogen bond flip of the HF moiety between the two oxygen atoms of acetate as indicated in Scheme 1. Especially form **C** will be subject to such a fast hydrogen bond flip, whereas the corresponding flip in form **D** will be slower. The flip may involve a transition state exhibiting a symmetric configuration with bifurcated hydrogen bond; however, such a symmetric structure cannot be excluded as main structure of the complex. Some of us have previously found evidence for similar very fast hydrogen bond flips in low-temperature solutions of hydrogen bonded complexes [24].

The question arises, whether the observed equilibrium between the high-temperature form **A** and the low-temperature form **B** can be explained in terms of the reaction network of Scheme 1. **A** dominates at higher and **B** at lower temperatures which means that **B** should exhibit a larger dipole moment than **A**. At 130 K, the interconversion rate is about $300\,s^{-1}$. As mentioned above, the interconversion is not related to hydrogen bond breaking processes which would lead to a coalescence of the signals of $[FHO]^-$ and $[FDO]^-$, in contrast to the experimental findings, nor to proton exchange, which would lead to a collapse of the $^1J(FH$ O) spin–spin splitting pattern. On the other hand, from the graphs of Fig. 6 there is no evidence for major changes of the hydrogen bond geometry. Therefore, the process is also not related to proton jumps between two sites in the hydrogen bond, one closer to F and the other closer to O. These constraints as well as the simple molecular structure of $[FHO]^-$ limit strongly the possibilities.

Thus, as a preliminary working hypothesis, we tentatively assign **A** to **C** and **B** to **D**. An argument against this assignment is that one expects very large rate constants of the interchange between forms **C** and **D**, in contrast to what is found for **A** and **B** experimentally. However, it may be that the dynamics of the interchange are determined by an unknown aggregation process involving not only complexes $[FHO]^-$ but also solvent molecules and the countercation. Depending on the aggregation state, the angle β may adopt a preferential value.

Authors would like to thank the referee for pointing out another mechanism, which could be responsible for the spectral changes shown in Fig. 4. In this mechanism **A** is $CH_3COOH\cdots F^-$ and **B** is $CH_3COO^-\cdots HF$, which differ only by the average proton position, while the dynamic behaviour is attributed to the slow solvent reorganization that is needed to convert one of these forms to the other. This attribution is supported by the continuous change of average q_1 values (see Table 4). Slow (in the NMR time scale) proton transfer, $CH_3COOH\cdots F^- \leftrightarrow CH_3COO^-\cdots HF$, can really be a reason of the observed NMR effects, but solvent reorganization as a process retarding the proton transfer is more than doubtful. Indeed, dielectric relaxation in non-viscous liquids takes usually the time as low as 10^{-10}–10^{-12} s, and low viscosity of the used freon mixture at 120–140 K is proved by comparatively sharp NMR lines of the solvent. More probable seems to be the process of slowing down, shown in Scheme 2.

Such interconversion involves not only proton transfer but also H-bond reorganization, which requires some activation energy for breaking down one of the hydrogen bonds. This hypothetical mechanism can be confirmed or rejected by a calculation of the whole reaction pathway.

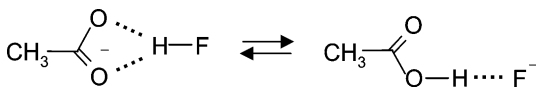

Scheme 2.

6. Conclusions

We have shown that using low-temperature NMR it is possible to detect non-trivial properties of simple hydrogen bonded clusters of fluoride with carboxylic acid. As fluoride and hydroxide have many similarities, this work may also be interesting for modeling complex hydrogen bonded networks in functional biomolecules. Using the valence bond order correlations, it is possible to link the worlds of NMR parameters and hydrogen bond geometries, and obtain information about the effects of a polar solvent on the latter. We hope that such results will stimulate further theoretical work in this area of research.

Acknowledgements

This work is financially supported by the Russian Foundation for Basic Research, Grants 03-03-32272 and 03-03-04009, the Deutsche Forschungsgemeinschaft, Bad Godesberg, and the Fonds der Chemischen Industrie, Frankfurt. P.M.T. thanks the Fonds for a Kékulé scholarship. Authors are grateful to the referee for valuable comments and suggestions.

References

[1] W.W. Cleland, M.M. Kreevoy, Science 264 (1994) 1887.
[2] P.A. Frey, S.A. Whitt, J.B. Tobin, Science 264 (1994) 1927.
[3] N.S. Golubev, G.S. Denisov, V.A. Gindin, S.S. Ligay, H.-H. Limbach, S.N. Smirnov, J. Mol. Struct. 322 (1994) 83.
[4] A.S. Mildvan, M.A. Massiah, T.K. Harris, G.T. Marks, D.H.T. Harrison, C. Viragh, P.M. Reddy, I.M. Kovach, J. Mol. Struct. 615 (2002) 163.
[5] C. Viragh, T.K. Harris, P.M. Reddy, M.A. Massiah, A.S. Mildvan, I.M. Kovach, Biochemistry 39 (2000) 16200.
[6] Y. Kim, K.H. Ahn, Theor. Chem. Acc. 106 (2001) 171.
[7] D.B. Northrop, Acc. Chem. Res. 34 (2001) 790.
[8] W.W. Cleland, Arch. Biochem. Biophys. 382 (2000) 1.
[9] K.B. Schowen, H.H. Limbach, G.S. Denisov, R.L. Schowen, Biochim. Biophys. Acta 1458 (2000) 43.
[10] B.A. Katz, J.R. Spencer, K. Elrod, C. Luong, R.L. Mackman, M. Rice, P.A. Sprengeler, D. Allen, J. Janc, J. Am. Chem. Soc. 124 (2002) 11657.
[11] P.A. Frey, J. Mol. Struct. 615 (2002) 153.
[12] (a) A. Warshel, A. Papazyan, P.A. Kollman, Science 269 (1995) 102. (b) A. Warshel, A. Papazyan, Proc. Natl Acad. Sci. USA 93 (1996) 13665. (c) A. Warshel, J. Biol. Chem. 273 (1998) 27035. (d) C.L. Perrin, J.B. Nielson, Annu. Rev. Phys. Chem. 48 (1997) 511.
[13] C.J. Smallwood, M.A. McAllister, J. Am. Chem. Soc. 119 (1997) 11277.
[14] G.A. Kumar, Y. Pan, C.J. Smallwood, M.A. McAllister, J. Comput. Chem. 19 (1998) 1345.
[15] N.S. Golubev, I.G. Shenderovich, P.M. Tolstoy, D.N. Shchepkin, J. Mol. Struct. (2004) (in press).
[16] I.G. Shenderovich, S.N. Smirnov, G.S. Denisov, V.A. Gindin, N.S. Golubev, A. Dunger, R. Reibke, S. Kirpekar, O.L. Malkina, H.-H. Limbach, Ber. Bunsen. Phys. Chem. 102 (1998) 422.
[17] I.G. Shenderovich, H.-H. Limbach, S.N. Smirnov, P.M. Tolstoy, G.S. Denisov, N.S. Golubev, Phys. Chem. Chem. Phys. 4 (2002) 5488.
[18] I.G. Shenderovich, A.P. Burtsev, G.S. Denisov, N.S. Golubev, H.-H. Limbach, Magn. Res. Chem. 39 (2001) S1/91.
[19] P.M. Tolstoy, P. Schah-Mohammedi, S.N. Smirnov, N.S. Golubev, G.S. Denisov, H.-H. Limbach, J. Am. Chem. Soc., submitted for publication.
[20] I.G. Shenderovich, P.M. Tolstoy, N.S. Golubev, S.N. Smirnov, G.S. Denisov, H.-H. Limbach, J. Am. Chem. Soc. 125 (2003) 11710.
[21] (a) L. Pauling, J. Am. Chem. Soc. 69 (1947) 542. (b) I.D. Brown, Acta Crystallogr. B48 (1992) 553.
[22] E. Bjarnov, W.H. Hocking, Z. Naturforsch. 33A (1978) 610.
[23] N.S. Golubev, E.G. Pushkareva, Vestnik LGU 11 (1985) 87.
[24] F. Männle, H.-H. Limbach, G.S. Denisov, J. Am. Chem. Soc., submitted for publication.